

在离子液体[BMIIm][BF₄]中电沉积光亮金镀层

宋云鹤 杨培霞 连 叶 冯忠宝 张锦秋 安茂忠*

(哈尔滨工业大学化工与化学学院, 城市水资源与水环境国家重点实验室, 哈尔滨 150001)

摘要: 在离子液体 1-丁基-3-甲基咪唑四氟硼酸盐 ([BMIIm][BF₄]) 中以 HAuCl₄·3H₂O 为主盐、通过添加 5,5-二甲基乙内酰脲 (DMH) 和胞嘧啶可得到色泽光亮、厚度达 1.5 μm 的金镀层, 沉积过程中阴极电流效率可达到 100%。SEM 和 XRD 测试结果表明, DMH 和胞嘧啶具有细化晶粒、平整镀层的作用。电化学测试结果表明, DMH 可分别与 Au³⁺、Au⁺ 形成配合物 [Au(DMH)₄]⁻、[Au(DMH)₂]⁻, 抑制了还原过程的表面转化步骤, 从而增加了阴极极化, 起到光亮镀层、细化晶粒的作用; 胞嘧啶可在金核表面吸附, 从而可以进一步光亮镀层、细化晶粒, 与 DMH 有协同作用。循环伏安测试研究了镀液的电化学行为, 研究表明在此体系中 Au³⁺ 的还原为两步还原过程, 分别为 Au³⁺ → Au⁺ 和 Au⁺ → Au。此外 DMH 和胞嘧啶的添加不会带来副反应。

关键词: 金镀层; 离子液体; 电沉积; 5-5 二甲基乙内酰脲; 胞嘧啶

中图分类号: O614.123; TQ153.1

文献标识码: A

文章编号: 1001-4861(2018)01-0142-09

DOI: 10.11862/CJIC.2018.020

Electrodeposition of Bright Gold Deposits in Ionic Liquid [BMIIm][BF₄]

SONG Yun-He YANG Pei-Xia LIAN Ye FENG Zhong-Bao ZHANG Jin-Qiu AN Mao-Zhong*

(State Key Laboratory of Urban Water Resource and Environment, School of Chemistry and
Chemical Engineering, Harbin Institute of Technology, Harbin 150001, China)

Abstract: A golden-yellow gold deposit with a thickness of 1.5 μm was electrodeposited from the bath with 5,5-dimethylhydantoin (DMH) as the complexing agent and cytosine as the additive in [BMIIm][BF₄] solution. The cathodic current efficiency was nearly 100% during electrodepositing. SEM and XRD results indicated that DMH and cytosine had significant effects on the surface morphologies and phase structure of the deposits. The grain size and roughness of gold deposits decreased adding DMH and cytosine into the bath. Moreover, the Au (111) plane also became more obvious. The influences of DMH and cytosine were studied by the linear sweep voltammetry (LSV). The gold complexes [Au(DMH)₄]⁻, [Au(DMH)₂]⁻ can be formed by DMH and Au³⁺, Au⁺, and the surface convert process was inhibited in the reduction process. The addition of DMH increased the cathodic polarization, which can brighten gold deposits and refine crystal grains of gold deposits. Cytosine was absorbed on Au nuclei, and it had synergistic effects with DMH on brightening gold deposits and refining crystal grains. Cyclic voltammetry (CV) was used to investigate the electrochemical behavior and the results revealed that the reduction of Au³⁺ to Au had a two-step reduction process. The first reduction process was Au³⁺ to Au⁺, and the second process was Au⁺ to Au, and the addition of DMH and cytosine did not bring side reactions.

Keywords: gold deposit; ionic liquid; electrodeposition; 5,5-dimethylhydantoin; cytosine

收稿日期: 2017-04-11。收修改稿日期: 2017-09-04。

国家自然科学基金(No.51474080)资助项目。

*通信联系人。E-mail: mzan@hit.edu.cn

0 Introduction

Gold deposits have numerous excellent physical and chemical properties, such as the golden yellow appearance, excellent electrical conductivity, topping thermal conductivity and outstanding chemical stability, and they are widely used as decorative deposits^[1], protective deposits^[2] and functional deposits^[3]. Gold deposits have extensive applications in decorations, electronic devices and aerospace. Gold electroplating baths including cyanide are the most widely used nowadays. Nowadays, cyanide baths, which have excellently stable electrolytes, refined grains and good adhesion of gold deposits^[4-5], are the most widely used gold electroplating. Unfortunately, cyanide brings immense hazards to the environment and biology^[6]. To solve the problem, golden-bright gold deposits were electrodeposited in ionic liquid 1-butyl-3-methylimidazolium tetrafluoroborate ([BMIIm][BF₄]), a free-cyanide bath.

Ionic liquids (ILs) are a kind of conductive organic compounds salt in liquid state at room temperature. Moreover, ILs have chemical stability, non-toxic, negligible vapor pressure, especially wide electrochemical window, high solubility of metal salts and high conductivity^[7-9]. Thus, ILs attract much attention in electrodeposition. Many active metals are unavailable in aqueous solution, but those can be obtained in ionic liquids by electrodeposition, such as Al^[10], Mg^[11], Na^[12] and Li^[13]. Ionic liquid [BMIIm][BF₄] has the excellent properties above mentioned, and it can be applied as a solvent in electroplating field^[14-15]. [BMIIm][BF₄] has a high solubility for chloroauric acid. The cations and anions of [BMIIm][BF₄] have no reducibility, so that Au³⁺ will not be reduced spontaneously. Therefore, [BMIIm][BF₄] was used as electrolytes for electrodeposition of gold in this work.

5,5-Dimethylhydantoin (DMH) has very important applications in electrodeposition, due to its low-cost, non-toxic and environmentally friendly properties. DMH can be used as a stable complexing agent in aqueous solution and it can combine with many metal ions to compose stable complexes, including Zn²⁺^[16],

Ag⁺^[17], Au³⁺^[18-19]. Therefore, DMH was added into [BMIIm][BF₄] as the complexing agent, and it had a good effect, as expected. However, the gold deposits obtained in the bath involving DMH as the complexing agent were insufficiently bright, whose surfaces were unsmooth. It was essential that appropriate additives were selected to improve the brightness of deposits and refine crystal grains. Cytosine can be used as an additive in metal electrodeposition, and it is adsorbed on the surface of electrodes^[20-21].

Bright gold deposits were obtained in IL by electrodeposition in this work, and there were some other studies carried out in ILs to electrodeposite gold. De Sá et al.^[22] electrodeposited gold deposits in 1-butyl-1-methyl-pyrrolidinium dicyanamide ionic liquid at open circuit and constant potential conditions. The grains of the deposits obtained in the two conditions were spherical and dendritic, respectively. The gold films obtained were golden-brown. Katayama et al.^[23] used 1-butyl-1-methylpyrrolidinium bis(trifluoromethylsulfonyl)amide as solvent, and gold tribromide was chosen as the main salt on this basis. The Au nano-particles with a diameter of 3 nm were obtained, which almost dispersed in the bath. The compact and bright gold deposits were not obtained in the work of other researchers.

In this work, [BMIIm][BF₄] was chosen as the solvent and chloroauric acid (HAuCl₄·3H₂O) as the main salt. DMH and cytosine were added into the baths as the complexing agent and the additive, respectively. The gold deposits obtained in the above-mentioned baths were characterized by scanning electron microscope (SEM) and X-ray diffraction (XRD). The influences of DMH and cytosine in the electrodeposition were investigated by linear sweep voltammetry (LSV). Furthermore, cyclic voltammetry (CV) were performed to study the electrochemical behavior of the baths.

1 Experimental

1.1 Materials and methods

[BMIIm][BF₄] was commercially available, and dried under vacuum for 24 h at 353 K before used.

$\text{HAuCl}_4 \cdot 3\text{H}_2\text{O}$ was added to $[\text{BMIm}][\text{BF}_4]$ with a concentration of $0.05 \text{ mol} \cdot \text{L}^{-1}$, which was prepared by Au and hydrochloric acid and nitric acid. A magnetic stirrer stirred the solution under dry N_2 at 328 K for 6 h until $\text{HAuCl}_4 \cdot 3\text{H}_2\text{O}$ added was completely dissolved. The baths with DMH (Aladdin, 98%) and cytosine (Aladdin, 98%) were prepared in the same way.

The surface morphology of gold deposits was characterized by scanning electron microscopy (SEM, Zeiss Supra55 SAPHIRE) at 10 kV. The crystal structure was investigated by X-ray diffractometry (XRD, Bruker D8 Advance) with $\text{Cu } K\alpha$ radiation at 40 kV and 40 mA ($\lambda=0.154 \text{ nm}$). The 2θ ranged from 20° to 90° at a scan rate of $0.02^\circ \cdot \text{s}^{-1}$. The type of counting X-ray was counts $\cdot \text{s}^{-1}$, and the detector used was LynxEye.

The electrochemical measurements including linear sweep voltammetry and cyclic voltammetry were carried out in N_2 atmosphere at 328 K. A three-electrode electrolytic cell and an electrochemical workstation CHI750d were used. A glassy carbon electrode (GCE, $\Phi=3 \text{ mm}$) was used as the working electrode (WE) of cyclic voltammetry. The WE was a glassy carbon rotating disk electrode (GC-RDE, $\Phi=5 \text{ mm}$) in linear sweep voltammetry. The reference electrode (RE) was a platinum wire ($\Phi=0.38 \text{ mm}$) and the counter electrode (CE) was a platinum plate ($1 \text{ cm} \times 1 \text{ cm}$) in the voltammetry measurements. The linear sweep voltammograms and cyclic voltammograms were separately performed at a scan rate of 1 and $10 \text{ mV} \cdot \text{s}^{-1}$. The GCE was successively polished by $\alpha\text{-Al}_2\text{O}_3$ polishing powder with particle size of $1.5 \mu\text{m}$, $1 \mu\text{m}$ and $0.5 \mu\text{m}$ after an electrochemical measurement was completed. Then, the GCE was washed with ethanol and deionized water in turn, and finally dried with N_2 .

1.2 Preparation and characterization of gold deposits

In the electrodeposition, a gold plate ($1.5 \text{ cm} \times 1.5 \text{ cm}$) was used as the anode, and a nickel-plated copper foil ($1.0 \text{ cm} \times 1.0 \text{ cm}$) was the cathode. The distance between the anode and the cathode was retained at 3 cm. The current density was carried out

$0.3 \text{ A} \cdot \text{dm}^{-2}$ for electrodeposition in N_2 atmosphere. A magnetic stirrer at a rate of $500 \text{ r} \cdot \text{min}^{-1}$ stirred the baths used in the electrodeposition at 328 K. After electrodeposition, the sample was successively rinsed with ethanol and deionized water to remove the remaining electrolyte, and then dried with N_2 .

The average grain size (t) of deposits was estimated using the Scherrer equation^[24]:

$$t = \frac{0.9\lambda}{B \cos \theta}$$

where λ is the wavelength of the incident X-rays, B is the peak half width at half maximum in radians, and θ is the Bragg angle.

The thickness of gold deposits and the cathodic current efficiency were calculated by the weight of gold deposits. The thicknesses of gold deposits were calculated according to the equation:

$$d = \frac{m_2 - m_1}{\rho S} \times 10^4$$

where d (μm) is the thickness of gold deposits, m_1 (g) and m_2 (g) are the weight of nickel-plated copper foils before and after the electrodeposition of gold, ρ is the density of gold ($19.32 \text{ g} \cdot \text{cm}^{-3}$), and S (cm^2) is the area of gold deposits.

The cathodic current efficiency was calculated according to the equation:

$$\eta = \frac{m_2 - m_1}{KIt}$$

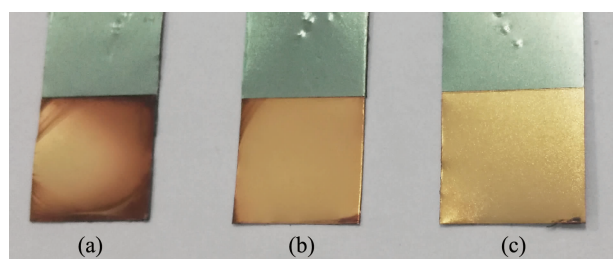
where η is the cathodic current efficiency, K is the electrochemical equivalent of Au^{3+} ($2.45 \text{ g} \cdot \text{A}^{-1} \cdot \text{h}^{-1}$), I (A) is the current in the electrodeposition process, and t (h) is the time of electrodeposition.

2 Results and discussion

2.1 Characterization of gold deposits

Gold deposits were obtained from $[\text{BMIm}][\text{BF}_4]$ solution without and with DMH, as well as the bath with DMH and cytosine. Fig.1 displays digital pictures of different gold deposits.

The gold deposit obtained in the basic bath is red-brown, whose surface is uneven and rough (Fig. 1a). As displayed in Fig.1b, the gold deposit with a relatively uniform surface was obtained in bath with DMH, whereas the colour is slightly red. Compared to



(a) Without DMH and cytosine, (b) With $0.3 \text{ mol} \cdot \text{L}^{-1}$ DMH,
(c) With $0.3 \text{ mol} \cdot \text{L}^{-1}$ DMH and $20 \text{ mmol} \cdot \text{L}^{-1}$ cytosine

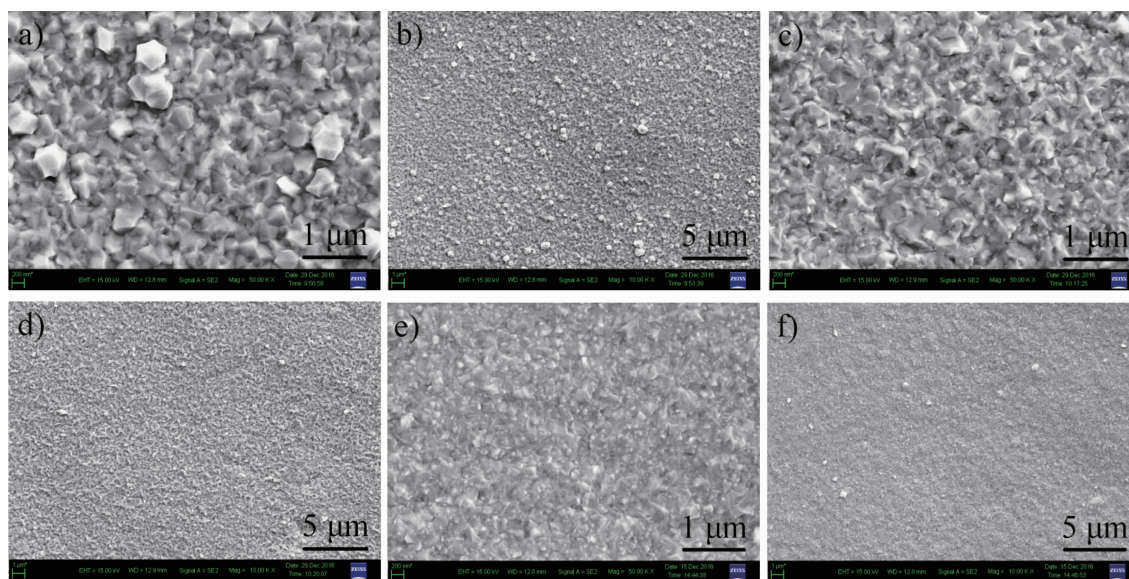
Fig.1 Digital pictures of gold deposits obtained from [BMI_m][BF₄] containing $\text{HAuCl}_4 \cdot 3\text{H}_2\text{O}$

the gold deposits in Fig.1a and b, the appearance of the gold deposit in Fig.1c is optimal. The gold deposit is bright golden yellow, and the surface is uniform. It indicates that the addition of DMH as the complexing agent and cytosine as the additive to the bath can significantly improve the appearance of gold deposits. The thicknesses of the gold deposits displayed in Fig. 1 are nearly $1.5 \mu\text{m}$. The corresponding cathodic current efficiencies are 100% in the electrodeposition. The result indicates that the cathode reaction was the reduction of Au^{3+} in bath with DMH and cytosine, and no other side reactions occurred.

Fig.2 reveals the surface morphologies of the gold deposits obtained in the [BMI_m][BF₄] solution without and with DMH, as well as the bath with DMH and

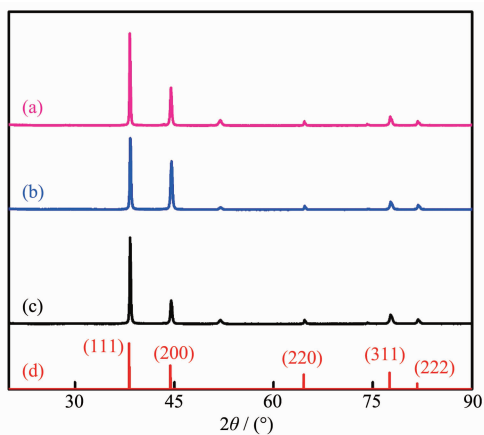
cytosine. As displayed in Fig.2a and b, the deposit obtained in the bath without DMH and cytosine is uneven, and many coarse crystal particles exist on the surface. The grains become smaller and the coarse crystal particles almost disappear on the surface, which is still uneven (Fig.2c and d). The gold deposit obtained in bath with DMH and cytosine is the smoothest, and the crystals are the smallest (Fig.2e and f). It can be concluded that gold deposits with a bright golden yellow appearance and refined grains can be obtained when DMH is added as the complexing agent and cytosine is added as the additive in the bath.

The XRD patterns of the gold deposits obtained in the above mentioned electrolytes are presented in Fig.3. The five peaks in Fig.3(a) and (b) and (c) at 2θ values of 38.2° , 44.4° , 64.6° , 77.6° and 81.8° are indexed to the Au (111), (200), (220), (311) and (222) crystal face, respectively. The two indexed peaks in Fig.3(a) and (b) and (c) at 2θ values of 51.9° and 74.1° correspond to the nickel-plated copper foil, which was used as the substrate of the electrodeposition of gold. As shown in Fig.3, the intensity of the diffraction peak corresponding to the Au (111) crystal face is the largest in the five peaks. It indicates that the gold electrodeposits were preferentially deposited along the direction



(a, b) Without DMH and cytosine, (c, d) With $0.3 \text{ mol} \cdot \text{L}^{-1}$ DMH, (e, f) With $0.3 \text{ mol} \cdot \text{L}^{-1}$ DMH and $20 \text{ mmol} \cdot \text{L}^{-1}$ cytosine

Fig.2 SEM images of gold deposits obtained from [BMI_m][BF₄] containing $\text{HAuCl}_4 \cdot 3\text{H}_2\text{O}$



(a) Without DMH and cytosine, (b) With $0.3 \text{ mol} \cdot \text{L}^{-1}$ DMH, (c) With $0.3 \text{ mol} \cdot \text{L}^{-1}$ DMH and $20 \text{ mmol} \cdot \text{L}^{-1}$ cytosine, (d) Au (PDF#04-0784)

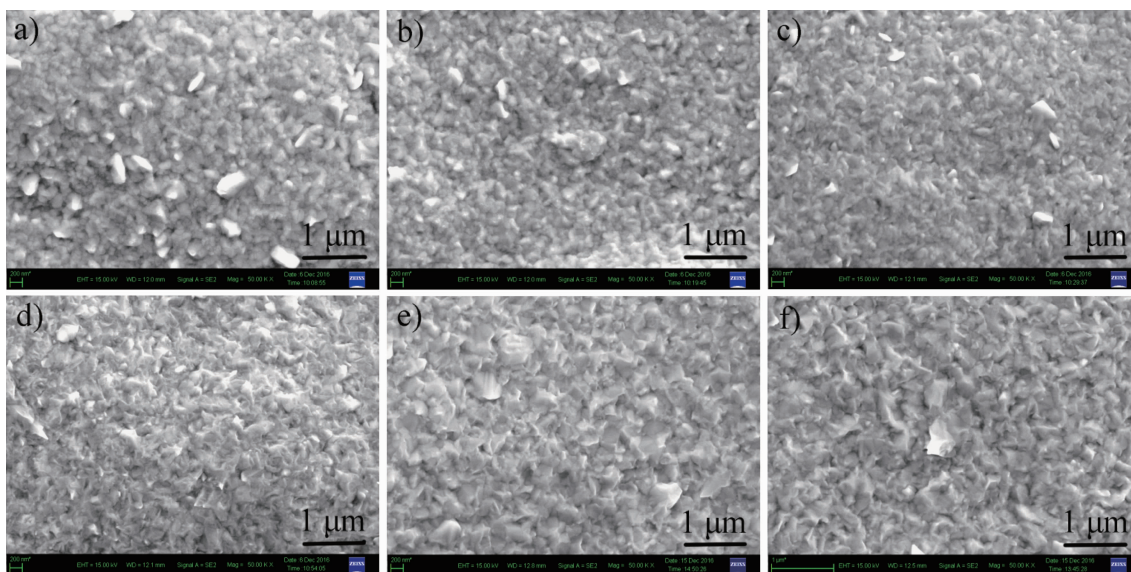
Fig.3 XRD patterns of gold deposits obtained from [BMIm][BF₄] containing $\text{HAuCl}_4 \cdot 3\text{H}_2\text{O}$

of the Au (111) crystal face. The tendency of preferred deposition along Au (111) crystal face direction is intenser with the addition of DMH and cytosine. The average size of crystal grains of gold deposits was calculated according to the Scherrer formula^[24]. The average size of crystal grains that Fig.3(a), (b) and (c) correspond to is 34.8, 30.7 and 28.1 nm, respectively. The grains of the deposits obtained in bath with DMH and cytosine are the smallest. This result is consistent with the SEM measurements.

2.2 Influences of different components

In order to investigate the influences of DMH, the gold deposits were obtained from the different solution of $0.05 \text{ mol} \cdot \text{L}^{-1} \text{HAuCl}_4 \cdot 3\text{H}_2\text{O}$ in [BMIm][BF₄] containing 0, 0.10, 0.20, 0.25, 0.3 and $0.40 \text{ mol} \cdot \text{L}^{-1}$ DMH, respectively, and then the macroscopic conditions of the gold deposits were observed. The color of the gold deposits obtained from the bath without DMH is brown-yellow, and the surface is reddish. The gold deposits obtained from the bath with $0.10, 0.20$ and $0.25 \text{ mol} \cdot \text{L}^{-1}$ DMH are all yellow. With adding DMH into the electrolytes, the appearances of gold deposits turn to better. The gold deposits obtained from the bath with $0.30 \text{ mol} \cdot \text{L}^{-1}$ DMH are obviously optimal in appearance, which possess a brighter surface; the color of the deposits doesn't change as the concentration of DMH continues to increase.

SEM measurements were performed to further investigate the influence of DMH on the surface morphologies of gold deposits. Fig.4 shows SEM images of the gold deposits obtained from the baths containing different concentrations of DMH. The surface of the gold deposits is rough, and there are many coarse crystal grains on the gold deposits (Fig. 4a). The smoothness of the gold deposits increases with the increased concentration of DMH, and the



(a) 0, (b) $0.10 \text{ mol} \cdot \text{L}^{-1}$, (c) $0.20 \text{ mol} \cdot \text{L}^{-1}$, (d) $0.25 \text{ mol} \cdot \text{L}^{-1}$, (e) $0.30 \text{ mol} \cdot \text{L}^{-1}$, (f) $0.40 \text{ mol} \cdot \text{L}^{-1}$

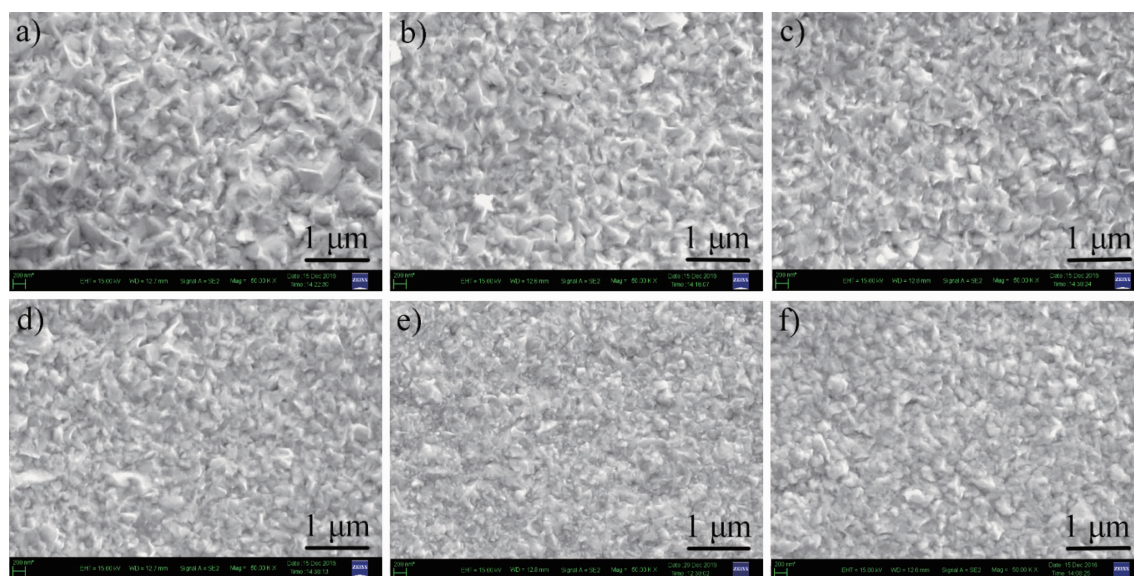
Fig.4 SEM images of gold deposits obtained from the bath containing $0.05 \text{ mol} \cdot \text{L}^{-1} \text{HAuCl}_4 \cdot 3\text{H}_2\text{O}$ with different concentrations of DMH

number of the coarse crystal grains is less and less. The gold deposits are the most smooth when the concentration of DMH is 0.30~0.40 mol·L⁻¹, and the coarse crystal grains almost disappear. It was proved that DMH could brighten the gold deposits and refine the crystal grains with the contrast of the macroscopic states and surface morphologies of the deposits.

The influences of cytosine on the gold deposits were investigated on the basis of DMH in the baths. Cytosine with a concentration of 5, 10, 15, 20 and 25 mmol·L⁻¹ was dissolved in the [BMI][BF₄] solution containing HAuCl₄·3H₂O and DMH. The gold deposits obtained in the baths with cytosine are brighter than those obtained in the bath without cytosine. The gold deposits obtained in the baths with cytosine are golden yellow, and almost no difference in appearance

can be observed with the increase of the concentration of cytosine.

The surface morphologies of the gold deposits were characterized by SEM measurements to research the influences of cytosine. The crystal grains of the gold deposits can be refined with adding cytosine (Fig. 5). The sizes of the crystal grains are gradually reduced with the concentration of cytosine increasing. The crystal grains of the gold deposits are the smallest, which were obtained in the bath with 20 mmol·L⁻¹ cytosine. SEM images indicated that cytosine could further refine the crystal grains of the gold deposits on the basis of DMH in the bath. Moreover, the addition of cytosine can enhance the brightness of the gold deposits through the contrast of the macroscopic states.



(a) 0, (b) 5 mmol·L⁻¹, (c) 10 mmol·L⁻¹, (d) 15 mmol·L⁻¹, (e) 20 mmol·L⁻¹, (f) 25 mmol·L⁻¹

Fig.5 SEM images of gold deposits obtained from the bath containing 0.05 mol·L⁻¹ HAuCl₄·3H₂O and 0.3 mol·L⁻¹ DMH with different concentrations of cytosine

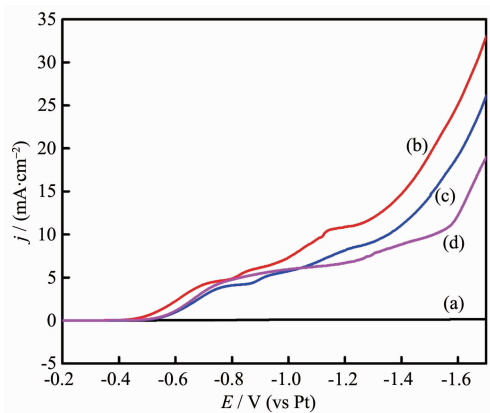
2.3 Electrochemical measurements

As shown in Fig.6 the linear sweep voltammograms were measured with scan rate of 1 mV·s⁻¹ at 328 K in order to further investigate the influences of DMH and cytosine in the bath. The potential was scanned from -0.2 V, along the negative potential direction up to -1.8 V. Fig.6a is the linear sweep voltammogram of the pure ionic liquid [BMI][BF₄]. The current density is less than 10⁻³ mA·cm⁻² in the

potential scan from -0.2 to -1.8 V. Therefore, [BMI][BF₄] is chemically stable in the above measurement conditions. The curves b, c and d are the voltammograms of the bath containing HAuCl₄·3H₂O without DMH and cytosine, with DMH, and with DMH and cytosine, respectively.

The current density of the curve b increases sharply from -0.45 V; with adding DMH, the potential shifts negatively to -0.53 V (Fig.6c). Besides, the

current density of the curve c decreases with the contrast of curve b. The gold complexes $[\text{Au}(\text{DMH})_4]^-$ may be formed by Au^{3+} and DMH in the bath, which can be formed in aqueous solutions^[18-19]. $[\text{Au}(\text{DMH})_4]^-$ inhibits the surface convert process in the reduction process, and it leads to the reduction of $[\text{Au}(\text{DMH})_4]^-$ occurring at more negative potential compared to Au^{3+} . Therefore, the addition of DMH increases the cathodic polarization, resulting in brightening gold deposits and refining crystal grains of gold deposits.



(a) Without $\text{H[AuCl}_4\cdot 3\text{H}_2\text{O}]$, (b) With $0.05 \text{ mol}\cdot\text{L}^{-1} \text{ H[AuCl}_4\cdot 3\text{H}_2\text{O}]$, (c) With $0.05 \text{ mol}\cdot\text{L}^{-1} \text{ H[AuCl}_4\cdot 3\text{H}_2\text{O}]$ and $0.3 \text{ mol}\cdot\text{L}^{-1} \text{ DMH}$, (d) With $0.05 \text{ mol}\cdot\text{L}^{-1} \text{ H[AuCl}_4\cdot 3\text{H}_2\text{O}]$ and $0.3 \text{ mol}\cdot\text{L}^{-1} \text{ DMH}$ and $20 \text{ mmol}\cdot\text{L}^{-1} \text{ cytosine}$; Scan rate: $1 \text{ mV}\cdot\text{s}^{-1}$; Temperature: 328 K

Fig.6 Linear sweep voltammograms recorded at the GC-RDE in $[\text{BMIm}][\text{BF}_4]$

The overpotential of curve d is not obviously changed with the addition of cytosine to the bath, but the cathodic current density is lower compared to the curve c when the potential exceeds -1.1 V . This period corresponds to the reduction of $[\text{Au}(\text{DMH})_2]^-$ to Au . (The detailed analysis of the reactions is investigated in Fig.8) Cytosine can be adsorbed on the generated Au nuclei^[20-21], which is related to the growth rate of crystal nucleus and the nucleation rate of deposits. The addition of cytosine inhibits the reduction of $[\text{Au}(\text{DMH})_2]^-$ to Au , leading to the current density decreasing. Cytosine can be used as an additive to brighten the deposits and refine the grains, which has a synergistic effect with DMH. It accords with the results of digital images, SEM and XRD measurements.

The cyclic voltammogram recorded at the GCE of

$[\text{BMIm}][\text{BF}_4]$ was performed with scan rate of $10 \text{ mV}\cdot\text{s}^{-1}$ at 328 K to define the electrochemical window. As shown in Fig.7, the chemical properties of $[\text{BMIm}][\text{BF}_4]$ are stable at the range of -2.0 to 1.9 V in the above conditions. A cathode peak occurs at around -1.0 V in the voltammogram curve, which may be caused by the oxidation of the resulting redazate during the potential scan along the negative direction.

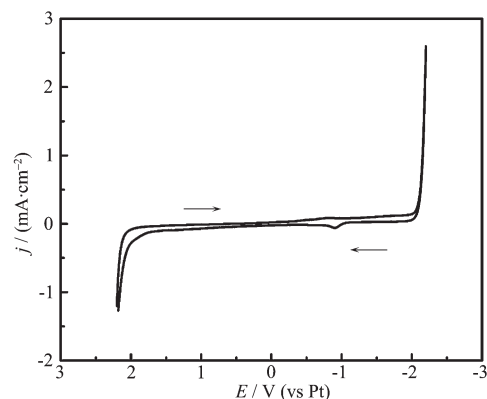
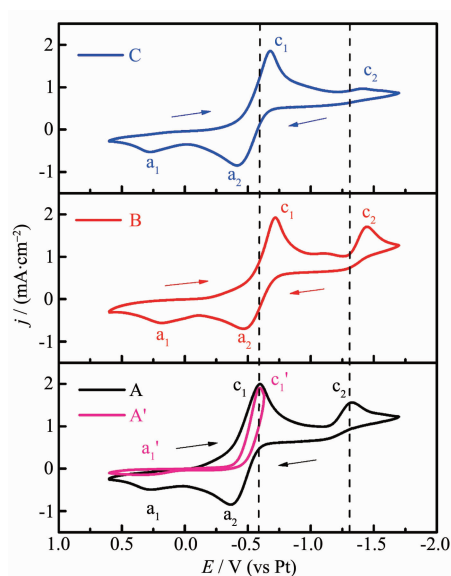


Fig.7 Cyclic voltammogram recorded at the GCE in $[\text{BMIm}][\text{BF}_4]$ with scan rate of $10 \text{ mV}\cdot\text{s}^{-1}$ at 328 K

Cyclic voltammograms were performed to investigate the electrochemical behavior of the bath containing $\text{H[AuCl}_4\cdot 3\text{H}_2\text{O}]$ in the absence or presence of DMH and cytosine, as shown in Fig.8. Fig.8A shows the cyclic voltammogram of the $[\text{BMIm}][\text{BF}_4]$ solution containing $\text{H[AuCl}_4\cdot 3\text{H}_2\text{O}]$. The potential was scanned from 0.6 V , along the negative potential direction up to -1.7 V , and then inverted to 0.6 V . Two reduction peaks (Fig.8A) are observed in the potential scan from 0.6 to -1.7 V vs Pt wire, at -0.59 V (c_1) and -1.3 V (c_2), respectively. The c_1 peak is attributed to the reduction of Au^{3+} to Au^+ , and the c_2 peak is assigned to the reduction of Au^+ to Au . The reactions the two reduction peaks (c_1 and c_2) represent are essentially consistent with the conclusions of previous authors^[25-26]. The curve A presents two oxidation peaks, a_1 and a_2 , in the reverse potential scan, which correspond to 0.27 and -0.36 V , respectively.

In order to investigate the reactions the two oxidation peaks (a_1 and a_2) corresponded to separately, the curve A' were performed. The potential was scanned from 0.6 V , along the negative potential



(A, A') without DMH and cytosine, (B) with 0.3 mol·L⁻¹ DMH, (C) with 0.3 mol·L⁻¹ DMH and 20 mmol·L⁻¹ cytosine; Scan rate: 10 mV·s⁻¹; Temperature: 328 K

Fig.8 Cyclic voltammograms recorded at the GCE in a solution of 0.05 mol·L⁻¹ HAuCl₄·3H₂O in [BMIIm][BF₄]

direction up to -0.63 V when the c_1' peak just emerged, and then inverted to 0.6 V. The c_1' peak represents the reduction of Au³⁺ to Au⁺, which is as same as the c_1 peak shown in Fig.8A. It is attributed to that the potentials of the c_1 peak in Fig.8A and c_1' peak in Fig.8A' are same in the completely same measurement conditions. Therefore, the a_1' peak is assigned to the oxidation of Au⁺ to Au³⁺. The a_1 peak and the a_2 peak separately correspond to the oxidation of Au⁺ to Au³⁺, Au to Au⁺. Based on the above conclusions, a gold plate was used as the anode to ensure the purity of the bath and maintain a certain concentration of Au³⁺ in the bath, which could be dissolved in the electrodeposition.

Fig.8B shows the cyclic voltammogram of the [BMIIm][BF₄] solution containing HAuCl₄·3H₂O and DMH. The corresponding potentials of the c_1 and c_2 peak are -0.72 V and -1.43 V (Fig.8B), respectively. The addition of DMH did not change the reactions in the bath, and the obvious difference is the negative shift of the two cathode peaks (c_1 and c_2). DMH may complex with Au³⁺ and Au⁺ to form [Au(DMH)₄]⁻ and [Au(DMH)₂]⁻ in the bath, which inhibit the two reduction

processes, respectively. The c_1 and c_2 peak correspond to the reduction of [Au(DMH)₄]⁻ to [Au(DMH)₂]⁻, [Au(DMH)₂]⁻ to Au (Fig.8B). DMH can increase the cathodic polarization, which is consistent with the results of Fig.6.

Fig.8C shows the cyclic voltammogram of the bath consisting of HAuCl₄·3H₂O and DMH and cytosine. Two cathodic peaks appear in the curve C, representing the same reduction reactions with those of the curve B, and the corresponding potentials are the same as those of the curve B. The comparison of the three curves indicates that no side reactions occurred when DMH and cytosine were added to the electrolyte, which was consistent with the cathodic current efficiency of 100%.

3 Conclusions

It is first time that the golden-yellow gold deposit with a thickness of 1.5 μm can be obtained in ionic liquid [BMIIm][BF₄] containing HAuCl₄·3H₂O and DMH and cytosine. DMH and cytosine had obvious effects on brightening deposits and refining grains. The optimum concentrations of DMH and cytosine were 0.3 mol·L⁻¹ and 20 mmol·L⁻¹, respectively. Linear sweep voltammograms and cyclic voltammograms indicated that DMH may coordinate with Au³⁺ and Au⁺, which increased the cathodic polarization, and the addition of cytosine on the basis of DMH could make the current density lower in the second reduction process, which was related to the adsorption of cytosine on the generated gold nuclei. The interaction between cytosine and DMH was synergism that made gold deposits bright and crystal grains refined. The cathodic current efficiency was 100%, indicating no side reactions occur, which can be confirmed by the cyclic voltammograms. Besides, cyclic voltammograms revealed that the reduction of Au³⁺ to Au in the bath was a two-step reduction process, including the reduction of Au³⁺ to Au⁺, and further, Au⁺ to Au.

References:

- [1] Dimitrijević S, Rajčić -Vujanović M, Alagić S, et al. *Electrochim. Acta*, 2013,104:330-336

- [2] Christie I R, Cameron B P. *Gold Bull.*, **1994**,**27**(1):12-20
- [3] Watanabe H, Hayashi S, Honma H. *J. Chem. Soc.*, **1999**,**146**(2):574-579
- [4] Kato M, Okinaka Y. *Gold Bull.*, **2004**,**37**(1/2):37-44
- [5] Green T A. *Gold Bull.*, **2007**,**40**(2):105-114
- [6] Sadyrbaeva T Z. *Sep. Sci. Technol.*, **2012**,**86**:262-265
- [7] Seddon K R. *J. Chem. Technol. Biotechnol.*, **1997**,**68**(4):351-356
- [8] Endres F, El Abedin S Z. *Chem. Chem. Phys.*, **2006**,**8**(18):2101-2116
- [9] Abbott A P, McKenzie K. *J. Phys. Chem. Chem. Phys.*, **2006**,**8**(37):4265-4279
- [10] Ueda M, Inaba R, Ohtsuka T. *Electrochim. Acta*, **2013**,**100**:281-284
- [11] Shimamura O, Yoshimoto N, Matsumoto M, et al. *J. Power Sources*, **2011**,**196**(3):1586-1588
- [12] Wibowo R, Aldous L, Rogers E I, et al. *J. Phys. Chem. C*, **2010**,**114**(8):3618-3626
- [13] Endres F. *ChemPhysChem*, **2002**,**3**(2):144-154
- [14] Yang P, Zhao Y, Su C, et al. *Electrochim. Acta*, **2013**,**88**:203-207
- [15] Eugenio S, Rangel C M, Vilar R, et al. *Electrochim. Acta*, **2011**,**56**(28):10347-10352
- [16] Pavlovich G Z, Luthy R G. *Water Res.*, **1988**,**22**(3):327-336
- [17] Liu A, Ren X, An M, et al. *Sci. Rep.*, **2014**,**4**:3837
- [18] Oyaizu K, Ohtani Y, Shiozawa A, et al. *Inorg. Chem.*, **2005**,**44**(20):6915-6917
- [19] Ren X, Song Y, Liu A, et al. *Electrochim. Acta*, **2015**,**176**:10-17
- [20] Lyu Z Y, Li A Q, Fei Y, et al. *Electrochim. Acta*, **2013**,**109**:136-144
- [21] Zhang Q L, Zhou D L, Li Y F, et al. *Microchim. Acta*, **2014**,**181**(11/12):1239-1247
- [22] De Sá A I, Eugénio S, Quaresma S, et al. *Surf. Coat. Technol.*, **2013**,**232**:645-651
- [23] Katayama Y, Endo T, Miura T, et al. *J. Electrochem. Soc.*, **2014**,**161**(3):D87-D91
- [24] Cullity B D. *Element of X-ray Diffraction*. Massachusetts: Addison-Wesley, **1978**:32-106
- [25] Xu X H, Hussey C L. *J. Electrochem. Soc.*, **1992**,**139**(11):3103-3108
- [26] Oyama T, Okajima T, Ohsaka T. *J. Electrochem. Soc.*, **2007**,**154**(6):D322-D327